ChemComm

Cocrystals of Li^+ Encapsulated Fullerenes and Tb(III) Double-Decker Single Molecule Magnet in a Quasi-Kagome Lattice

Journal:	*ChemComm*
Manuscript ID	CC-COM-06-2020-004349.R1
Article Type:	Communication

COMMUNICATION

Cocrystals of Li^+ Encapsulated Fullerenes and Tb(III) Double-Decker Single Molecule Magnet in a Quasi-Kagome Lattice

Received 00th January 20xx,
Accepted 00th January 20xx

DOI: 10.1039/x0xx00000x

Hikaru Iwami,[a] Junfei Xing,[b] Ryo Nakanishi,[b] Yoji Horii,‡*[b] Keiichi Katoh,*[a] Brian K. Breedlove,[a] Kazuhiko Kawachi,[c] Yasuhiko Kasama,[c] Eunsang Kwon,[d] and Masahiro Yamashita*[a,b,e,f]

Cocrystallization of a lithium ion encapsulated fullerene $Li^+@C_{60}$ with a terbium(III) phthalocyaninato porphyrinato double-decker single-molecule magnet [Tb(Pc)(OEP)] is reported. The cocrystal, containing PF_6^- as a counter anion, packs in a quasi-kagome lattice, which leads to intermolecular ferromagnetic interactions as well as the modulation of the single-molecule magnet (SMM) properties.

Single-molecule magnets (SMMs)[1] have unique magnetic bistabilities on the molecular level, making them useful in ultra-high density molecular memories, quantum computing and molecular spintronics.[2] In particular, lanthanoid ion-based SMMs have high operating temperatures because of large spin-orbital coupling and ligand field splitting.[3, 4] In addition, terbium(III)-bis(tetrapyrrole) double-decker complexes are known to be excellent SMMs with large activation energies for spin reversal (~400 cm^{-1} for the bis(phthalocyaninato)-terbium(III) double-decker complex $TbPc_2$).[3] Not only the electronic structures of the isolated molecules but also the crystal packings of SMMs greatly affect the magnetic properties. Katoh *et. al.* have reported that 1D packing of $TbPc_2$ analogues along a magnetic easy axis enhances the SMM properties.[5] Controlling the packing structures is an effective way to induce intermolecular magnetic dipole-dipole interactions. In 2014, three kinds of cocrystals composed of (phthalocyaninato)-(porphyrinato)-dysprosium(III) double-decker complexes Dy(Pc)(TClPP) and C_{60} were reported,[6] and their SMM properties were modulated by subtly changing the molecular structures and crystal packings. From detailed analyses of the association of the multiple-decker complexes and the fullerene derivatives,[7] new SMM-nanocarbon hybrid materials have been prepared. Some endohedral lanthanofullerenes have been reported to show unique magnetic properties, such as strong lanthanoid-radical exchange interactions[8, 9] and excellent SMM properties.[10] Our group has recently reported that lanthanofullerene-carbon nanotube hybrid material shows enhanced SMM properties originating from SMM-SMM interactions.[11] Not only purely organic fullerenes but also metal encapsulated fullerene derivatives have become available for cocrystallization. Lithium-ion-encapsulated fullerene $Li^+@C_{60}$ is commercially available owing to improved synthetic methods.[12] Various unique properties of $Li^+@C_{60}$, such as high ionic conductivity,[13] enhancement of chemical reactivity,[14] and use as a dopant in perovskite solar cells,[15] have been reported so far. In addition, motion of the Li^+ ion in the C_{60} cage has been analyzed by using NMR analysis, X-ray structural analysis,[16] terahertz spectroscopy and heat capacity analyses.[17, 18] Moreover, the C_{60} cage of $Li^+@C_{60}{\cdot}PF_6^-$ is basically neutral,[19] enabling the control of the crystal packing by changing the counter anion. However, cocrystallization of $Li^+@C_{60}$ and double-decker complexes has not been reported so far.

In this work, we report the cocrystallization of $Li^+@C_{60}$ with the terbium(III) double-decker complex Tb(Pc)(OEP), which contains 2,3,7,8,12,13,17,18-octaethylporphyrinato (OEP) and phthalocyaninato (Pc) ligands. In addition, we present the structures of new cocrystals of Tb(Pc)(OEP) with C_{70} and C_{60} units. The OEP unit interacted with fullerene derivatives,[20] forming five different cocrystals: $[Tb(Pc)(OEP)]_3(Li^+@C_{60}{\cdot}PF_6^-)_2$ (**1**), [Tb(Pc)(OEP)] ($Li^+@C_{60}{\cdot}BF_4^-$) (**2**), [Tb(Pc)(OEP)](C_{70}) (**3**), [Tb(Pc)(OEP)](C_{60})(C_6H_{14}) (**4**) and [Tb(Pc)(OEP)](C_{60})(Et_2O) (**5**). All cocrystals were characterized by using X-ray structural analyses and magnetic properties measurements. **1** packs in a quasi-kagome lattice arrangement in which the Tb(III) ions are located on the vertex of the triangle, resulting in intermolecular ferromagnetic interactions.

[a] Department of Chemistry, Graduate School of Science, Tohoku University, 6-3, Aramaki-Aza-Aoba, Aoba-ku, Sendai 980-8578, Japan
[b] WPI Research Center, Advanced Institute for Materials Research, Tohoku Univbersity, 2-1-1 Katahira, Aoba-Ku, Sendai 980-8577, Japan
[c] Idea International Co., Ltd., 1-15-35 Sagigamori, Aoba-ku, Sendai 981-0922, Japan
[d] Research and Analytical Center of Giant Molecules, Tohoku University, 6-3, Aramaki-Aza-Aoba, Aoba-ku, Sendai 980-8578, Japan
[e] Center for Spintronics Research Network (CSRN), Tohoku University, 2-1-1 Katahira, Aoba-Ku, Sendai 980-8577, Japan
[f] School of Materials Science and Engineering, Nankai University, Tianjin 300350, China
† Electronic Supplementary Information (ESI) available.
‡ Present address: Department of Chemistry, Faculty of Science, Nara Women's University, Nara 630-8506, Japan

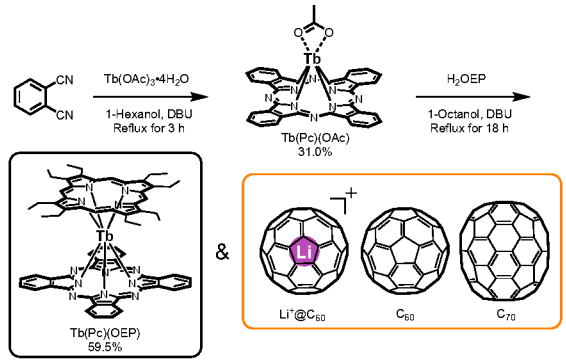

Scheme 1 Synthesis and molecular structures in this work.

Tb(Pc)(OEP) was synthesized by reacting a mononuclear Tb(III)-Pc-acetate complex Tb(Pc)(OAc) with metal-free H_2OEP in the presence of a base catalyst (Scheme 1). Cocrystals of $Li^+@C_{60}$ and Tb(Pc)(OEP) were grown via vapor diffusion of ethyl ether (poor solvents) into a mixture of $Li^+@C_{60}$, Tb(Pc)(OEP) and an excess amount of the counter anion in *o*-dichlorobenzene. Cocrystals **1** and **2** were obtained by using PF_6^- and BF_4^- as the counter anions, respectively. In both cases, the positions of the Li^+ ions could not be determined because of the low electron density and motion of the Li^+ ions even at low temperature.[16, 17] In addition, rotational disorder in the C_{60} cages was found in the crystal structures of **1** and **2**.

Cocrystal **1** crystallized in the orthorhombic space group $Cmc2_1$. Two crystallographically inequivalent Tb(Pc)(OEP) units and $Li^+@C_{60}$ units are arranged in a 2D layer in the *ab*-plane. A $Li^+@C_{60}$ unit is surrounded by three Tb(Pc)(OEP) units. One of the $Li^+@C_{60}$ is coordinated by two OEP and one Pc, and the other is coordinated by one OEP and two Pc ligands. Therefore, the Tb(III) ions are arranged in two kinds of isosceles triangles (triangles A and B on Fig. 1a), of which side lengths ranged from 12.678 to 13.911 Å in the packing of **1**. The vertexes of each triangle are shared with neighbouring triangles, forming a quasi-kagome lattice.

In **2**, Tb(Pc)(OEP) and $Li^+@C_{60}$ units stacked alternately to form a 1D column along the *a*-axis (Fig. 1b). Similar 1D packing has been reported in cocrystals of Pc multiple-decker complexes and C_{60} by Jiang *et al.*[6] and Katoh *et al.*[7] The inter- and intracolumn Tb(III)-Tb(III) distances were 15.189 and 13.880 Å, respectively.

To synthesize **3**–**5**, a mixture of Tb(Pc)(OEP) and the fullerene derivatives C_{70} and C_{60} dissolved in the halobenzene (*o*-dichlorobenzene or 1,2,4-trichlorobenzene) was diffused to the poor solvent (hexane or diethyl ether). Cocrystal **3** was composed of Tb(Pc)(OEP) units and C_{70} units, both of which stacked alternately to form 1D columns along the *b*-axis (Fig. 1c). The crystal packing of **3** resembles that of **2**. However, the bulky C_{70} units and the absence of BF_4^- ions causes the intra- and intercolumn Tb(III)-Tb(III) distances longer and shorter (15.507 Å and 13.664 Å), respectively. C_{60} and Tb(Pc)(OEP) were cocrystallized by diffusing an *o*-dichlorobenzene solution into hexane to obtain **4**. **4** is composed of dimerized Tb(Pc)(OEP) and dimerized C_{60} units which are stacked alternately, forming AABB-type slipped columns in the [101] direction (Fig. 1d). Cocrystal **5** was obtained from diffusion into diethyl ether (Et_2O). The crystal packing of **5** is similar to that of **4**, although some of the solvent molecules were Et_2O in **5** (Fig. 1e).

It is known that the face-to-face distance (*r*) between OEP and Pc correlates with the redox states of Tb(Pc)(OEP).[21] The oxidation of the ligands of the double-decker complexes decreases the face-to-face electrostatic repulsion of the π-

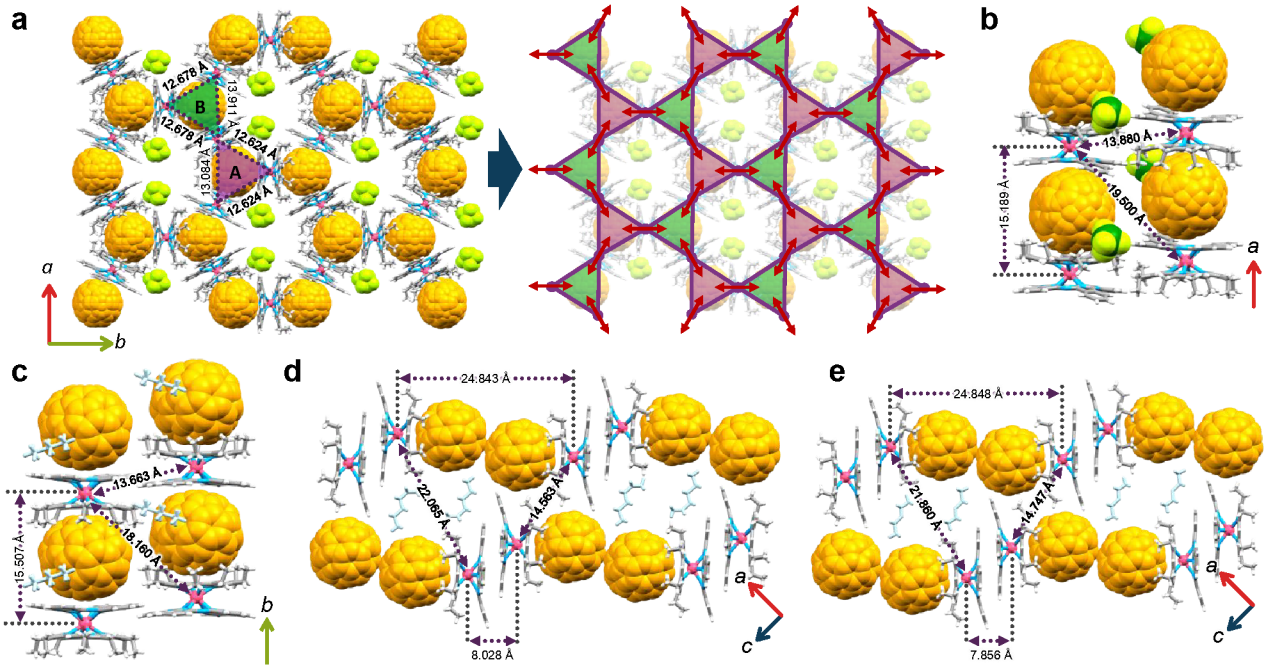

Fig. 1. Packing structure of (a) **1** (b) **2**, (c) **3**, (d) **4** and (e) **5**. Numbers on the figures are calculated intermolecular Tb(III)-Tb(III) distances. Counter anions and solvent molecules are shown in light green and light blue, respectively. Red arrows near the Tb(III) ions in Fig. 1 (a) represent possible directions of the spins.

ligands, making the *r* value shorter. The *r* values for the cocrystals are summarized in Table S2. In each cocrystal, the *r* values are shorter than those in crystals of neutral Tb(Pc)(OEP) (Table S4) because of the chemical pressures induced by the fullerene derivatives. In addition, the *r* values in **1** and **2** are shorter than those in cocrystals containing C_{70} and C_{60}, indicating that the electron withdrawing character of $Li^+@C_{60}$ decreases the electron repulsion between Pc and OEP among the Tb(Pc)(OEP) units. The twist angles between the Pc and the OEP ligands (θ) were close to 45° (Fig. S1 and Table S2).[22] This means that coordination geometries around the Tb(III) ions are close to square-antiprismatic (SAP) geometries, which are ideal for SMMs.[22]

DC magnetic susceptibility measurements were performed on **1**–**5**. $\chi_M T$ values at room temperature are close to the theoretical value for a Tb(III) ion (11.81 cm^3 K mol^{-1}). For **1** and **2**, $\chi_M T$ increased in the low temperature region, indicating that there are intermolecular ferromagnetic interactions. To validate the ferromagnetic interactions between the Tb(III) ions in **1**, two kinds of isosceles triangle units (triangle A and B in Fig. 1a) were picked and the magnetic dipole-dipole energy among three Tb(III) ions (*E*) were calculated using the following equation:

$$E = E_{12} + E_{23} + E_{31}$$

E is the sum of the magnetic dipole-dipole energy of a pair of Tb(III) ions (E_{ij}) in the triangle, and E_{ij} is written as follows:

$$E_{ij} = -\frac{\mu_0}{4\pi r_{ij}^3}\{3(\boldsymbol{m}_i \cdot \boldsymbol{e}_{ij})(\boldsymbol{m}_j \cdot \boldsymbol{e}_{ij}) - \boldsymbol{m}_i \cdot \boldsymbol{m}_j\}$$

where r_{ij} is the distance between two Tb(III) ions, $\boldsymbol{m}_i$ and $\boldsymbol{m}_j$ are the magnetic moments of the Tb(III) ions, and $\boldsymbol{e}_{ij}$ is the unit vector connecting two Tb(III) ions. For simplicity, $\boldsymbol{m}_i$ and $\boldsymbol{m}_j$ were set to the vector connecting the centroids of the Pc and OEP ligands of the Tb(Pc)(OEP) units. In other words, $\boldsymbol{m}_i$ and $\boldsymbol{m}_j$ are the vectors perpendicular to the Pc and OEP plane. In addition, norms of $\boldsymbol{m}_i$ and $\boldsymbol{m}_j$ were set to $-g_J\mu_B J_z$, where g_J is the Lande *g*-factor (g_J = 1.5 for Tb(III)), and J_z is the *z*-components of the total angular momentum. In general, J_z is ±6 for Tb(III) double-decker complexes.[3] This simplified Ising model is only valid when the magnetic easy axis is perpendicular to the Pc and OEP plane. The energy diagrams for the spin configurations of the Tb(III)-triangles in **1** are shown in Fig. 3a. For both triangles, there should be doublet ground states, first quartet excited states, and second doublet excited states. The second doublet excited state is antiferromagnetically arranged with a small magnetic moment perpendicular to the triangle plane (*c*-axis in the crystal packing). In contrast, ground and first excited states have ferromagnetic spin configurations, affording a large magnetic moment in the *ab*-plane, of which the magnitude is ~10 times larger than those along the *c*-axis (Fig. S22). Thus, the interlayer magnetic interactions should be small. $\chi_M T$ values were simulated in a 1 kOe field using the spin configuration, and they slightly increased with a decrease in *T* to ~10 K because of the magnetic dipole-dipole interactions (Fig. 3b). The decrease in $\chi_M T$ values with a further decrease in temperature is due to the magnetic anisotropy of Tb(III) ions, which was overestimated in the present model. The magnitude of the increase in the $\chi_M T$ values is much smaller than that in the experimental data because only the discrete triangles were considered in the calculations. The quasi-kagome lattice configuration of the spins with a large resultant magnetic moment (Fig. 3c) could be modeled by combining the ground state spin configurations of triangles A and B. These ferromagnetic spin configurations appears to have a role in increasing the $\chi_M T$ values.

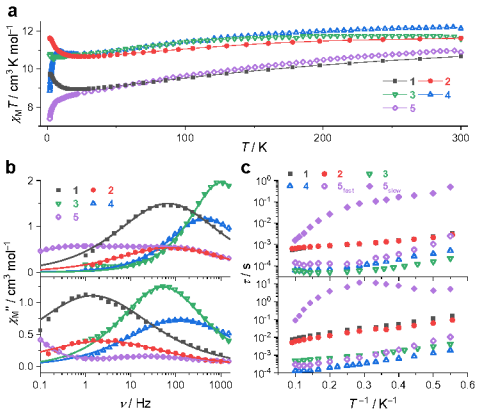

Fig. 2 (a) $\chi_M T$ vs *T* plots for **1**–**5** in a 1 kOe dc magnetic field. (b) χ_M'' vs ν plots for **1**–**5** at 2 K in the absence (upper) and in the presence (lower) of a dc magnetic field. (c) Temperature dependence of τ in the absence (upper) and presence (lower) of the dc magnetic field.

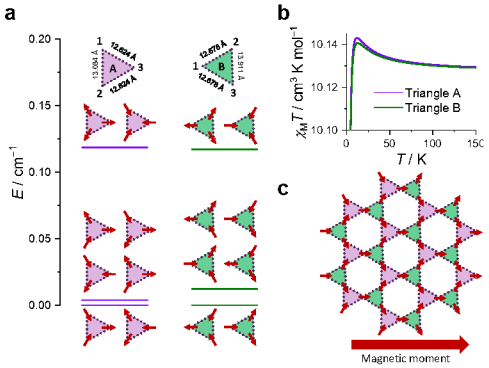

Fig. 3 (a) Energy diagrams of the spin configurations of triangles A and B in a zero dc magnetic field. Red arrows represent the spin directions. The ground and first excited states adopt ferromagnetic spin configurations with large magnetic moments in the triangle plane, whereas the second excited states take an antiferromagnetic spin configuration with a tiny magnetic moment perpendicular to the triangle plane. (b) Calculated $\chi_M T$ vs *T* plots for triangles A and B in a 1 kOe field. (c) A ground spin configuration for the quasi-kagome lattice.

In the case of **2**, the stacking along the *a*-axis induces ferromagnetic interactions (head-to-tail arrangement of the magnetic dipole). Although interchain magnetic dipole-dipole interactions should be antiferromagnetic because of the parallel arrangement of the spins, the columns are separated from each other due to the steric effects from BF_4^-. Therefore, the $\chi_M T$ values increase in the low temperature region because of the ferromagnetic arrangement of the spins among the columns. In contrast to **1** and **2**, the $\chi_M T$ values of the other cocrystals did not increase. For **3**, since the Tb(Pc)(OEP) units are separated from each other because of the bulky C_{70}, the

intermolecular Tb(III)-Tb(III) interactions in **3** should be weaker than those in the other cocrystals as evidenced by the temperature independent $\chi_M T$ values at low temperature. For **4** and **5**, the $\chi_M T$ values decreased in the low temperature region, which is due to the antiferromagnetic interactions among the dimerized Tb(Pc)(OEP) units.

To determine dynamic magnetic properties, alternative current (ac) magnetic measurements were performed (Figs. S5–S21). For all cocrystals, out-of-phase (χ_M'') signals were frequency (ν) dependent in the absence of a dc magnetic field, indicating that the Tb(Pc)(OEP) units act as SMMs. For **1**–**4**, a single peak was observed in χ_M'' vs ν plots, which was analysed using a generalized Debye model (Eq. S1a and S1b). For **5**, dual peaks (fast and slow relaxations) were fitted using an extended Debye model (Eq. S2a and S2b). Application of a dc bias field (2 kOe for **1**–**4** and 3 kOe for **5**) caused the χ_M'' peak to shift toward the lower ν region. This means that the quantum tunnelling of the magnetisation (QTM) in the doublet ground state can be suppressed. As shown in Fig. 2c, **1** and **2** have longer τ values than **3** and **4** do. The slower τ value for **5** is the longest among the present cocrystals. Our results indicate that the ac magnetic properties of the Tb(Pc)(OEP) units can be modulated via cocrystallization. Although the mechanism for the drastic changes in the spin dynamics is currently being investigated, the intermolecular ferromagnetic interactions in **1** and **2** likely act as an exchange-bias,[23] which suppresses QTM and elongates τ.

In conclusion, a series of cocrystals composed of heteroleptic Tb(III) double-decker complex and various fullerene derivatives were synthesized and characterized by using single crystal X-ray diffraction analyses and magnetic measurements. For cocrystals containing $Li^+@C_{60}$ (**1** and **2**), different counter anions resulted in different crystal packings. In particular, **1** was found to have a unique quasi-kagome lattice packing which induces intermolecular ferromagnetic interactions. Depending on the crystallization conditions, different packings, i.e., 1D column packings for **2** and **3** and AABB-type arrays of Tb(Pc)(OEP) and C_{60} dimers for **4** and **5,** formed. In addition, the magnetic properties of the Tb(Pc)(OEP) units were modulated via cocrystallization. Our results provide information for constructing new SMM-nanocarbon hybrid materials.

Conflicts of interest

There are no conflicts to declare.

Acknowledgement

This work was supported by CREST, JST (JPMJCR12L3), JSPS KAKENHI Grant Numbers JP20225003, JP15K05467, JP24750119, the Ministry of Education, Culture, Sports, Science, and Technology, Japan (MEXT). M. Y. thanks the support from the 111 Project (B18030) from China.

Notes and references

1 R. Sessoli, D. Gatteschi, A. Caneschi and M. A. Novak, *Nature*, 1993, **365**, 141-143.
2 L. Bogani and W. Wernsdorfer, *Nat. Mater.*, 2008, **7**, 179-186.
3 N. Ishikawa, M. Sugita, T. Ishikawa, S.-y. Koshihara and Y. Kaizu, *J. Am. Chem. Soc.*, 2003, **125**, 8694-8695.
4 F.-S. Guo, B. M. Day, Y.-C. Chen, M.-L. Tong, A. Mansikkamäki and R. A. Layfield, *Angew. Chem. Int. Ed.*, 2017, **56**, 11445-11449.
5 K. Katoh, S. Yamashita, N. Yasuda, Y. Kitagawa, B. K. Breedlove, Y. Nakazawa and M. Yamashita, *Angew. Chem. Int. Ed.*, 2018, **57**, 9262-9267.
6 H. Wang, K. Qian, D. Qi, W. Cao, K. Wang, S. Gao and J. Jiang, *Chem. Sci.*, 2014, **5**, 3214-3220.
7 K. Katoh, N. Yasuda, M. Damjanović, W. Wernsdorfer, B. K. Breedlove and M. Yamashita, *Chem. Eur. J.*, 2020, **26**, 4805-4815.
8 M. K. Singh, N. Yadav and G. Rajaraman, *Chem. Commun.*, 2015, **51**, 17732-17735.
9 G. Velkos, D. S. Krylov, K. Kirkpatrick, X. Liu, L. Spree, A. U. B. Wolter, B. Büchner, H. C. Dorn and A. A. Popov, *Chem. Commun.*, 2018, **54**, 2902-2905.
10 R. Westerström, J. Dreiser, C. Piamonteze, M. Muntwiler, S. Weyeneth, H. Brune, S. Rusponi, F. Nolting, A. Popov, S. Yang, L. Dunsch and T. Greber, *J. Am. Chem. Soc.*, 2012, **134**, 9840-9843.
11 R. Nakanishi, J. Satoh, K. Katoh, H. Zhang, B. K. Breedlove, M. Nishijima, Y. Nakanishi, H. Omachi, H. Shinohara and M. Yamashita, *J. Am. Chem. Soc.*, 2018, **140**, 10955-10959.
12 H. Okada, T. Komuro, T. Sakai, Y. Matsuo, Y. Ono, K. Omote, K. Yokoo, K. Kawachi, Y. Kasama, S. Ono, R. Hatakeyama, T. Kaneko and H. Tobita, *RSC Adv.*, 2012, **2**, 10624-10631.
13 H. Ueno, K. Kokubo, Y. Nakamura, K. Ohkubo, N. Ikuma, H. Moriyama, S. Fukuzumi and T. Oshima, *Chem. Commun.*, 2013, **49**, 7376-7378.
14 H. Ueno, H. Kawakami, K. Nakagawa, H. Okada, N. Ikuma, S. Aoyagi, K. Kokubo, Y. Matsuo and T. Oshima, *J. Am. Chem. Soc.*, 2014, **136**, 11162-11167.
15 I. Jeon, H. Ueno, S. Seo, K. Aitola, R. Nishikubo, A. Saeki, H. Okada, G. Boschloo, S. Maruyama and Y. Matsuo, *Angew. Chem. Int. Ed.*, 2018, **57**, 4607-4611.
16 S. Aoyagi, E. Nishibori, H. Sawa, K. Sugimoto, M. Takata, Y. Miyata, R. Kitaura, H. Shinohara, H. Okada, T. Sakai, Y. Ono, K. Kawachi, K. Yokoo, S. Ono, K. Omote, Y. Kasama, S. Ishikawa, T. Komuro and H. Tobita, *Nat. Chem.*, 2010, **2**, 678-683.
17 H. Suzuki, M. Ishida, M. Yamashita, C. Otani, K. Kawachi, Y. Kasama and E. Kwon, *Phys. Chem. Chem. Phys.*, 2016, **18**, 31384-31387.
18 H. Suzuki, M. Ishida, C. Otani, K. Kawachi, Y. Kasama, E. Kwon, Y. Miyazaki and M. Nakano, *Phys. Chem. Chem. Phys.*, 2019, **21**, 16147-16153.
19 Y. Yamada, A. V. Kuklin, S. Sato, F. Esaka, N. Sumi, C. Zhang, M. Sasaki, E. Kwon, Y. Kasama, P. V. Avramov and S. Sakai, *Carbon*, 2018, **133**, 23-30.
20 T. Ishii, N. Aizawa, R. Kanehama, M. Yamashita, K.-i. Sugiura and H. Miyasaka, *Coord. Chem. Rev.*, 2002, **226**, 113-124.
21 S. Takamatsu and N. Ishikawa, *Polyhedron*, 2007, **26**, 1859-1862.
22 S. Sakaue, A. Fuyuhiro, T. Fukuda and N. Ishikawa, *Chem. Commun.*, 2012, **48**, 5337-5339.
23 W. Wernsdorfer, N. Aliaga-Alcalde, D. N. Hendrickson and G. Christou, *Nature*, 2002, **416**, 406-409.

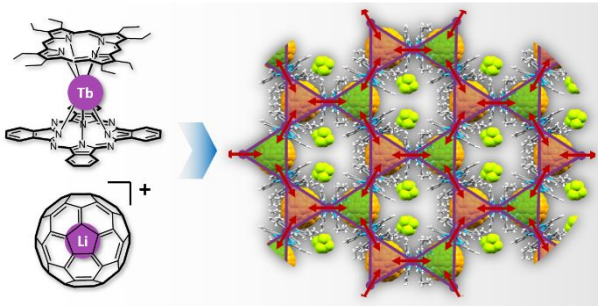

Cocrystallization of a lithium ion encapsulated fullerene with a terbium(III) phthalocyaninato porphyrinato double-decker single-molecule magnet results in a quasi-kagome lattice packing showing ferromagnetic spin arrangement.